

| | |
|--------------|--|
| Title | Variation of Crystallization Mechanisms in Flash-Lamp-Irradiated Amorphous Silicon Films |
| Author(s) | Ohdaira, Keisuke; Nishikawa, Takuya; Matsumura, Hideki |
| Citation | Journal of Crystal Growth, 312(19): 2834-2839 |
| Issue Date | 2010-06-25 |
| Type | Journal Article |
| Text version | author |
| URL | http://hdl.handle.net/10119/9885 |
| Rights | NOTICE: This is the author's version of a work accepted for publication by Elsevier. Keisuke Ohdaira, Takuya Nishikawa, and Hideki Matsumura, Journal of Crystal Growth, 312(19), 2010, 2834-2839, http://dx.doi.org/10.1016/j.jcrysgr.2010.06.023 |
| Description | |

Variation of Crystallization Mechanisms in Flash-Lamp-Irradiated Amorphous Silicon Films

Keisuke Ohdaira^{1,2}, Takuya Nishikawa¹, and Hideki Matsumura¹

¹Japan Advanced Institute of Science and Technology (JAIST)

1-1 Asahidai, Nomi, Ishikawa 923-1292, Japan

²PRESTO, Japan Science and Technology Agency (JST)

4-1-8 Honcho, Kawaguchi, Saitama 332-0012, Japan

Abstract

Flash lamp annealing (FLA) can form polycrystalline silicon (poly-Si) films with various microstructures depending on the thickness of precursor amorphous Si (a-Si) films due to the variation of crystallization mechanisms. Intermittent explosive crystallization (EC) takes place in precursor a-Si films thicker than approximately 2 μm , and the periodicity of microstructure formed resulting from the intermittent EC is independent of the thickness of a-Si films if their thickness is 2 μm or greater. In addition to the intermittent EC, continuous EC and homogeneous solid-phase crystallization (SPC) also occur in thinner films. These crystallization mechanisms are governed by the ignition of EC at Si film edges and the homogeneous heating of interior

a-Si. The results obtained in this study could be applied to control the microstructures of flash-lamp-crystallized poly-Si films.

Keywords: A1. Growth models, A1. Recrystallization, B2. Semiconducting silicon, B3.

Solar cells, A1. Surface structure, A1. Nucleation

PACS: 81.10.Jt, 81.40.Ef, 84.60.Jt, 81.16.Dn

1. Introduction

The rapid spread of photovoltaics has been demanded from the viewpoint of future energy and environmental issues, and the development of productive and cost-effective solar cells is one of the most important tasks. For cost reduction in crystalline silicon (c-Si) solar cells, which have a current market share of approximately 90% [1], the utilization of thin (<100 μm) wafers has been extensively investigated [2-4]. However, no one has yet established the methods of forming such thin wafers by cutting c-Si ingots with high yield and low kerf loss. Another approach to form thin c-Si is the utilization of thin Si films deposited on low-cost substrates, and a number of researchers have proposed various methods to form thin c-Si films, e.g. crystallization of deposited precursor amorphous Si (a-Si) films by annealing [5-8], and epitaxial growth of c-Si films on thin large-grain c-Si seed layers [9]. Although high throughput and low damage to low-cost substrates with poor thermal tolerance are necessary for the formation of thin c-Si, most of the methods do not meet these requirements. One way to form high quality c-Si films without thermal damage to substrates is to selectively heat a-Si films (keeping substrate temperature sufficiently low), in which the annealing duration for crystallization becomes quite important.

Flash lamp annealing (FLA), which is flash discharge from a xenon lamp array,

can realize an annealing duration on the order on milliseconds [10,11], corresponding to the thermal diffusion lengths of a-Si and glass of several tens of μm . This means that a precursor a-Si film of a few μm thickness, required for c-Si for the effective absorption of sunlight, can be fully heated and crystallized, while a glass substrate of ~ 1 mm thickness is not entirely heated. Also, FLA can heat a large-area substrate simultaneously without scanning process. Therefore, FLA can be a candidate method of forming c-Si films with high throughput and low thermal damage to substrates. We have succeeded in forming polycrystalline Si (poly-Si) films of more than 4 μm thickness by FLA of a-Si films even on conventional soda lime glass substrates [12], and demonstrated the operation of solar cells using flash-lamp-crystallized (FLC) poly-Si films [13,14]. The solar cell properties obtained so far are short-circuit current density of 8.6 mA/cm^2 , open-circuit voltage of 0.30 V, fill factor of 0.51, and conversion efficiency of 1.3% [14], and they will be improved by optimizing the solar cell process. We have also observed curious lateral crystallization in FLA, so called “explosive crystallization (EC)”, driven by the emission of heat generated due to phase transition from metastable a-Si to stable c-Si phases [15,16]. The characteristic lateral crystallization leaves behind periodic structures with a spacing of approximately 1 μm both on the surfaces of FLC poly-Si films and inside them, spontaneously formed

during FLA. The mechanisms of the emergence of such periodic structures and the controllability of the microstructures have not been fully clarified. Such fundamental understanding of crystallization mechanisms and the properties of FLC poly-Si films formed are necessary for the future application of FLC poly-Si films in photovoltaic technologies.

In this study, we have investigated the impact of precursor a-Si film thickness on the crystallization mechanisms and the microstructures of FLC poly-Si films. We have found that periodic structures tend to disappear in thin a-Si films, indicating the existence of different crystallization types depending on the thickness of a-Si films.

2. Experimental procedures

We first deposited a-Si films of 1.3-2.4 μm thickness by catalytic chemical vapor deposition (Cat-CVD) on $20\times 20\times 0.7\text{ mm}^3$ -sized quartz substrates with or without Cr coating. We have already confirmed that there is no significant difference in the crystalline fractions and microstructures of poly-Si films formed on quartz and soda lime glass substrates [12], and in this study, we chose quartz substrate (with a smaller thermal expansion coefficient) because it suppresses Si film peeling. The use of Cr films is also to suppress Si film peeling, and we have confirmed that Cr films do not

affect the crystallization mechanisms of a-Si films on them, except for a slight modulation of the irradiance required for crystallization caused by the reflection of irradiated flash lamp light on the Cr films. The Cat-CVD can produce a-Si films with low stress and low hydrogen content of approximately 3 atomic percent, and thus, is suitable as a method of depositing thick a-Si films capable of being crystallized without hydrogen bubbling. Detailed deposition conditions of a-Si films have been summarized elsewhere [17]. Only one shot of flash lamp light, with a broad spectrum mainly in the visible range [11], was irradiated for each sample. Irradiance of flash lamp light was tuned around 18-25 J/cm² in order to obtain as large an area of poly-Si as possible and to avoid the peeling of the Si film. No dehydrogenation process was performed prior to FLA. No additional heating of samples was performed during FLA. The microstructures of FLC poly-Si films were observed by differential optical microscopy, atomic force microscopy (AFM), and cross-sectional transmission electron microscopy (TEM). Crystallinity of Si films was characterized by Raman spectroscopy using a He-Ne laser of 632.8 nm wavelength. Raman spectra obtained were calibrated using the 520.5 cm⁻¹ line of a Si wafer. The full width at half maximum (FWHM) of a Si wafer was 4 cm⁻¹.

3. Results

Figure 1 shows surface appearances of FLC poly-Si films with various film thicknesses. A 2.4- μm -thick poly-Si film reveals a rainbow-colored surface, as previously shown on the surfaces of thicker FLC poly-Si films [12,15,16]. Figure 2 shows the surface differential microscopy images of FLC poly-Si films with thicknesses of 2.4 μm , shown in Fig. 1(a), and of 4.5 μm for comparison, shown in Fig. 1(b). One can clearly see characteristic periodic surface microstructures in both images. The microstructures are formed spontaneously during crystallization, and act as optical gratings to form rainbow-colored surfaces. The spacing of the periodic structures is approximately 1 μm , which is constant in spite of differing thicknesses of FLC poly-Si films. We can therefore conclude that the spacing of periodic structure is independent of the thickness of precursor a-Si films, if a-Si films have the same properties and if crystallization takes place in the same manner. Understanding the impact of a-Si film properties on periodic microstructures is also a quite important and interesting work, and we will tackle this investigation in the near future. Poly-Si films of 1.5 and 1.75 μm thicknesses also show the signature of lateral EC in the directions indicated by arrows in Fig. 1, but appear different from thicker FLC poly-Si films. The difference of surface colors originating from optical interference on the poly-Si surfaces indicates

the formation of different surface microstructures. This fact suggests that the 1.5-1.75 μm -thick poly-Si films are formed through a different crystallization mechanism from thicker films. Interestingly, crystallized areas close to a-Si/c-Si boundaries, indicated by dashed-line circles in Fig. 1, reveal different surface appearance from other crystallized parts, probably indicating the existence of different lateral crystallization mechanisms even in one sample. Moreover, the crystallized part of a poly-Si film of 1.3 μm thickness has no characteristic surfaces, and shows no evidence of lateral crystallization. These facts indicate that the thickness of precursor a-Si films has a significant impact on whether and how EC occurs.

Figure 3 shows AFM images of different areas of the surface of a 1.5 μm -thick FLC poly-Si film. The poly-Si surface located far from an a-Si/c-Si boundary, as shown in Fig. 3(a), has an entirely different microstructure from that of thicker FLC poly-Si films. The root-mean-square (RMS) roughness of the surface is estimated to be 26 nm, which is significantly greater than that of precursor a-Si films of about 2 nm [18]. The drastic increase in RMS roughness could not be caused through complete solid-phase crystallization, and thus, probably suggests the melting of a-Si during FLA. On the other hand, one can observe periodic microstructures with a pitch of approximately 1 μm on the surface close to an a-Si/c-Si boundary, as shown in Fig. 3(b).

This microstructure is similar to that of thicker FLC poly-Si films. The RMS roughness of the poly-Si surface is about 32 nm, which is much lower than that of thicker FLC poly-Si films of approximately 120 nm.

Figure 4 shows cross-sectional TEM images of a 1.75- μm -thick poly-Si film observed below the periodic and unperiodic microstructures. Both structures contain 100 nm-sized grains and a number of voids in the vicinity of their surfaces. Similar structures are seen below surface projections in thicker FLC poly-Si films (referred to as “region L” in a previous report [15]). Although a poly-Si film with unperiodic microstructures consists entirely of “region L”, a poly-Si film with periodic surface microstructures contains other characteristic regions with a periodicity of approximately 1 μm that have no voids inside, indicated by arrows in Fig. 4(b). These structures are similar to those included also in thicker FLC poly-Si films between region L’s, which only consists of 10-nm-sized fine grains and has been referred to as “region F” [15]. These facts suggest that EC with a similar mechanism also partially occurs in the observed poly-Si films.

Figure 5(a) shows normalized Raman spectra of FLC poly-Si films of 1.3-2.4 μm thicknesses. All the spectra have strong peaks at around 520 cm^{-1} originating from c-Si phases, and a-Si-related signals are hardly seen, indicating high crystalline fractions.

The Raman shift of the c-Si peak of a 1.3 μm -thick poly-Si film is 517.3 cm^{-1} , which is lower than the value of a c-Si wafer and indicates the existence of considerable tensile stress in the poly-Si film. On the other hand, Raman shifts of c-Si peaks of thicker poly-Si films are located close to that of a c-Si wafer, suggesting the formation of relaxed poly-Si films. Figure 5(b) shows FWHMs of c-Si peaks as a function of poly-Si film thickness. The c-Si peak of the 1.3 μm -thick poly-Si film, crystallized uniformly, has an FWHM of 6.8 cm^{-1} , which is smaller than those of poly-Si films formed through EC. The two poly-Si regions with different surface morphologies, shown in poly-Si films of 1.5 and 1.75 μm thicknesses, indicate different FWHMs, and poly-Si with periodic microstructures tends to show smaller FWHMs than that without periodic structures.

4. Discussion

We first review the previous understanding of EC observed in thick FLC poly-Si films. Crystallization starts from the edges, because the edge a-Si receives more flash lamp light than the interior. Once crystallization takes place at the edges, thermal emission due to a phase transition from metastable a-Si to stable c-Si occurs, and the heat emitted diffuses into neighboring a-Si areas, which induces further crystallization,

and resulting lateral movement of the crystallization front toward the inside. Crystallization takes place through the combination of solid-phase nucleation (SPN) and liquid-phase epitaxy (LPE) in the area close to a crystallization front receiving significant thermal diffusion, whereas SPN dominates crystallization in the areas with a greater distance from a crystallization front and not heated as much as closer areas, resulting in intermittent EC and the formation of regions L and F. Further quantitative discussion has been summarized elsewhere [15].

The ignition of lateral crystallization at film edges occurs when the temperature of the edges (T_{edge}) exceeds a threshold temperature for crystallization (T_{crys}). Figure 6 schematically shows the relation of temperatures between T_{edge} and the temperature of interior a-Si (T_{int}) at the moment that T_{edge} reaches T_{crys} during FLA, in the cases of thick and thin Si films. A thinner Si film should have lower thermal gain at the film edges than a thicker film because of a smaller edge area. Therefore, at the moment that T_{edge} reaches T_{crys} , the T_{int} of a thinner a-Si film becomes higher than that of a thicker film, which could induce different crystallization mechanisms. If T_{int} is high enough, the lateral crystallization could take place not intermittently but continuously, since a-Si with high T_{int} crystallizes within a shorter time in receiving thermal diffusion and emits heat immediately to neighboring a-Si. This is probably the reason for the

absence of periodic structures in thinner explosively crystallized poly-Si films. A high T_{int} also results in the formation of poly-Si consisting only of region L, formed through SPN and LPE. According to these considerations, intermittent EC could appear also in a thinner Si film in the final stage of a flash lamp pulse, at which T_{int} significantly decreases, as schematically shown in Fig. 7. The two different microstructures seen in 1.5 and 1.75 μm -thick poly-Si films are evidence of the variations in crystallization mechanism. As mentioned above, RMS roughness of 32 nm observed on the periodic microstructure of the 1.5- μm -thick poly-Si film is much less than that of approximately 120 nm on the surface of a 4.5- μm -thick FLC poly-Si film. This might be related to insufficient formation of region F in the thinner poly-Si film. One of the possible reasons for the formation of surface projections is high compressive stress applied to a Si film during FLA, due to selective heating of a Si film, and the compressive stress would be concentrated on deformable melted areas. In the case of completely intermittent EC observed in thicker Si films, melted areas are limited in the vicinity of the crystallization front due to low T_{int} , and melted areas, that is, region L, drastically projects upward. On the other hand, the EC observed in thinner films seems not to be completely intermittent since region F's do not penetrate to the Si/substrate interface, which is probably due to still higher T_{int} than that of thicker films. This incomplete

formation of region F's causes the widening of melted areas and less significant concentration of compressive stress, resulting in smaller surface deformation.

One may guess that a-Si could be crystallized without the assistance of lateral thermal diffusion if T_{int} increases sufficiently for crystallization simply by homogeneous flash irradiation. According to the discussion above, such a homogeneous crystallization should tend to occur in thinner films in which the ignition of EC at film edges is more difficult, and in fact, the interior part of 1.3- μm -thick Si films are crystallized with no significant surface deformation and no evidence of the lateral movement of the crystallization front. The reason for the peeling of Si at the edges might be high stress during EC. That is to say, EC occurs from the film edges, and homogeneous crystallization also takes place in the interior a-Si before the arrival of crystallization fronts.

The crystallization mechanisms considered above give us a valid explanation for the difference of FWHM in poly-Si formed through different crystallization patterns. As has been discussed in a previous work, nucleation occurs only through SPN [15], and the frequency of SPN dramatically increases with increasing temperature [19]. In the case of continuous EC shown in 1.5-1.75 μm -thick films, a Si film has momentarily the highest T_{int} among the three cases. Although 100-nm-sized large grains exists in

the films, probably grown through LPE, there should also be a huge number of finer nuclei formed through frequent SPN, and the finer grains dominate FWHM of a Raman spectrum. In contrast, T_{int} during intermittent EC should be lower than that during continuous EC, and thus, shallower FWHM of a c-Si Raman peak, meaning the existence of larger nuclei, is quite reasonable because of less frequent SPN. In the case of homogeneous crystallization observed in a 1.3- μm -thick poly-Si film, T_{int} during SPN should be lower than that during EC because there is no lateral thermal diffusion, which results in much less frequent SPN and the formation of larger grains. The large low-energy shift of a c-Si Raman peak can also be accounted for based on the differences of crystallization mechanisms. Poly-Si formed through EC undergoes partial melting during crystallization, which could induce stress relaxation, whereas no chance of relaxing stresses is given for homogeneously crystallized films, and tensile stress remains in the films.

Finally, we will discuss the possibility of controlling crystallization patterns and poly-Si microstructures by means other than change in Si film thickness, based on the findings in this study. The difficulty of creating EC in thin Si films arises due to insufficient thermal gain at film edges for the ignition of crystallization. This problem would be solved by applying additional local heating of a-Si, such as laser irradiation,

for the intentional ignition of crystallization. The control of crystallization patterns in thicker films is more challenging. We have not succeeded in forming poly-Si films through continuous EC because a Si film peels off during FLA with an irradiance higher than that needed for intermittent EC, even with the help of a Cr adhesion film. Further improvement in the adhesiveness of Si films onto substrates is necessary for the realization of poly-Si films with different microstructures.

5. Conclusion

FLA can crystallize a-Si films to form poly-Si films with a variety of microstructures, which are dominated by the ignition of crystallization at film edges and T_{int} . The periodicity of microstructures in poly-Si films formed through intermittent EC is independent of precursor a-Si film thickness. The periodic microstructures tend to disappear in thinner poly-Si films, due to higher T_{int} and resulting emergence of continuous EC instead of intermittent EC. Homogeneous crystallization is also possible by homogeneous heating of interior a-Si sufficient for crystallization without assistance of lateral thermal diffusion. Grain size inside films also corresponds to their crystallization mechanisms. The results obtained can be a guiding principle for the control of microstructures in FLC poly-Si films.

Acknowledgment

We would like to thank Mr. Owada and Mr. Yokomori of Ushio Inc. for the expert operation of the FLA system. We also thank Mr. Fukuda, Mr. Nishizaki, Ms. Abe, Mr. Endo and Ms. Fujiwara for the preparation of precursor a-Si films, and Professor M. A. Mooradian for improvement of English. This work was supported by Japan Science and Technology Agency (JST) PRESTO program.

References

- [1] I. Kaizuka, G. Watt, P. Hüsler, P. Cowley, R. Bründlinger, in: Proceedings of the 24th European Photovoltaic Solar Energy Conference, 2009, p.4501.
- [2] F. Dross, A. Milhe, J. Robbelein, I. Gordon, P. Bouchard, G. Beaucarne, J. Poortmans, in: Conference Record of 33rd IEEE Photovoltaic Specialists Conference, 2008, p.1584.
- [3] F. Henley, S. Kang, Z. Liu, L. Tian, J. Wang, Y. L. Chow, in: Proceedings of the 24th European Photovoltaic Solar Energy Conference, 2009, p.890.
- [4] M. Schumann, M. Singh, T. O. Pérez, S. Riepe, in: Proceedings of the 24th European Photovoltaic Solar Energy Conference, 2009, p.1222.
- [5] M. J. Keevers, T. L. Young, U. Schubert, M. A. Green, in: Proceedings of the 22nd European Photovoltaic Solar Energy Conference, 2007, p.1783.
- [6] T. Matsuyama, M. Tanaka, S. Tsuda, S. Nakano, Y. Kuwano, *Jpn. J. Appl. Phys.* 32 (1993) 3720.
- [7] S. Janz, M. Kuenle, S. Lindekugel, E. J. Mitchell, S. Reber, in: Conference Record of 33rd IEEE Photovoltaic Specialists Conference, 2008, p.168.
- [8] J. K. Saha, K. Haruta, M. Yeo, T. Koabayshi, H. Shirai, *Sol. Energy. Mat. Sol. Cells* 93 (2009) 1154.
- [9] A. G. Aberle, *J. Cryst. Growth* 287 (2006) 386.
- [10] M. Smith, R. McMahon, M. Voelskow, D. Panknin, W. Skorupa, *J. Cryst. Growth* 285 (2005) 249.

- [11] H. Habuka, A. Hara, T. Karasawa, M. Yoshioka, Jpn. J. Appl. Phys. 46 (2007) 937.
- [12] K. Ohdaira, T. Fujiwara, Y. Endo, S. Nishizaki, H. Matsumura, Jpn. J. Appl. Phys. 47 (2008) 8239.
- [13] Y. Endo, T. Fujiwara, K. Ohdaira, S. Nishizaki, K. Nishioka, H. Matsumura, Thin Solid Films (in press)
- [14] K. Ohdaira, T. Fujiwara, Y. Endo, K. Shiba, H. Takemoto, H. Matsumura, Jpn. J. Appl. Phys. 49 (2010) 04DP04.
- [15] K. Ohdaira, T. Fujiwara, Y. Endo, S. Nishizaki, H. Matsumura, J. Appl. Phys. 106 (2009) 044907.
- [16] H. D. Geiler, W. Glaser, G. Gotz, and M. Wagner, J. Appl. Phys. 59 (1985) 3091.
- [17] K. Ohdaira, S. Nishizaki, Y. Endo, T. Fujiwara, N. Usami, K. Nakajima, H. Matsumura, Jpn. J. Appl. Phys. 46 (2007) 7198.
- [18] K. Ohdaira, K. Shiba, H. Takemoto, T. Fujiwara, Y. Endo, S. Nishizaki, Y. R. Jang, H. Matsumura, Thin Solid Films 517 (2009) 3472.
- [19] C. Spinella and S. Lombardo, J. Appl. Phys. 84 (1998) 5383.

Figure captions

Fig. 1 Surface appearances of FLC poly-Si films with various film thicknesses. The size of the substrates is $20 \times 20 \text{ mm}^2$. Indications “a”, “c”, and “x” represent a-Si, poly-Si, and peeled areas, respectively. Arrows indicates possible lateral crystallization directions.

Fig. 2 Surface differential microscopy images of FLC poly-Si films with thicknesses of (a) $2.4 \text{ }\mu\text{m}$ and (b) $4.5 \text{ }\mu\text{m}$.

Fig. 3 AFM images of the surfaces of a $1.5 \text{ }\mu\text{m}$ -thick FLC poly-Si film observed in areas with different surface appearances.

Fig. 4 Cross-sectional TEM images of a $1.75\text{-}\mu\text{m}$ -thick poly-Si film observed below (a) unperiodic and (b) periodic microstructures. Protection films were formed just prior to the thinning of the sample for TEM observation.

Fig. 5 (a) Normalized Raman spectra of FLC poly-Si films with thicknesses of $1.3\text{-}2.4 \text{ }\mu\text{m}$. (b) FWHM of Raman c-Si peaks as a function of poly-Si film thickness. The error bars were estimated from Gaussian fitting errors.

Fig. 6 Schematic of the relation of temperatures between T_{edge} and T_{int} at the moment that T_{edge} reaches T_{crys} during FLA in the cases of thick and thin Si films. Due to the small thermal gain at Si film edges, more irradiance of flash lamp light is needed for

$T_{\text{edge}}=T_{\text{crys}}$, which results in higher T_{int} in a thinner film.

Fig. 7 Schematic view of the time-dependent intensity of flash lamp light and resulting variation of T_{int} .

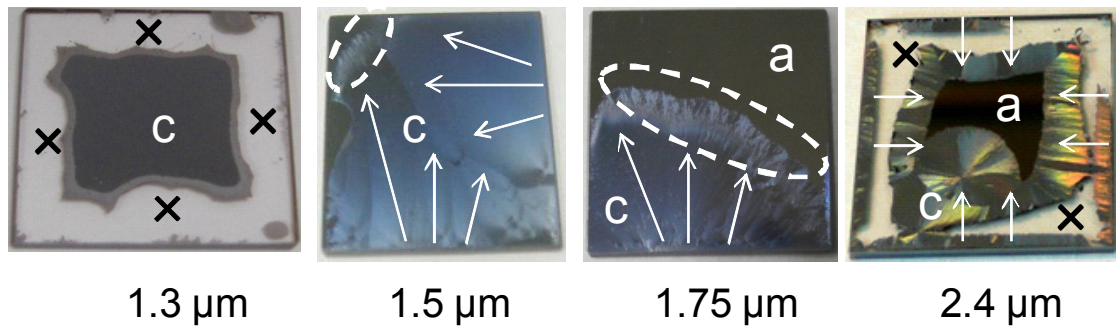


Fig. 1 K. Ohdaira *et al.*,

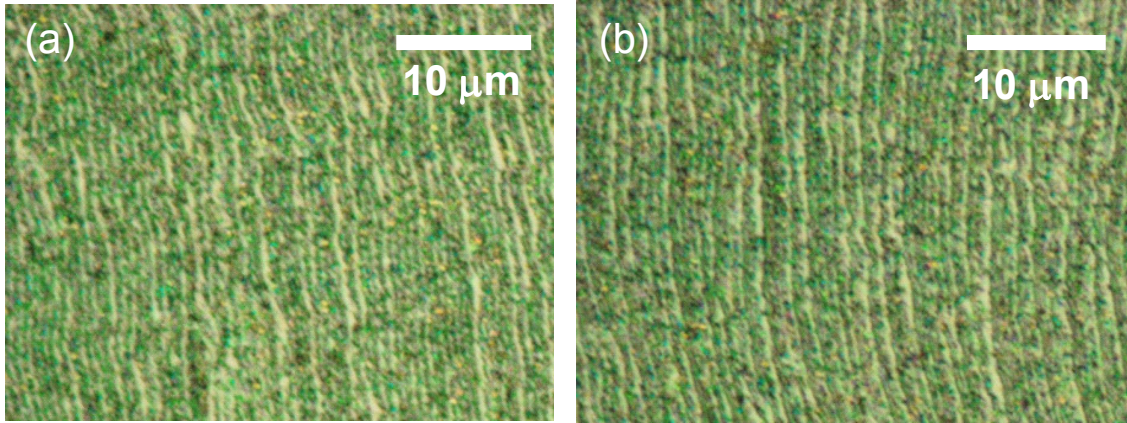


Fig. 2 K. Ohdaira *et al.*,

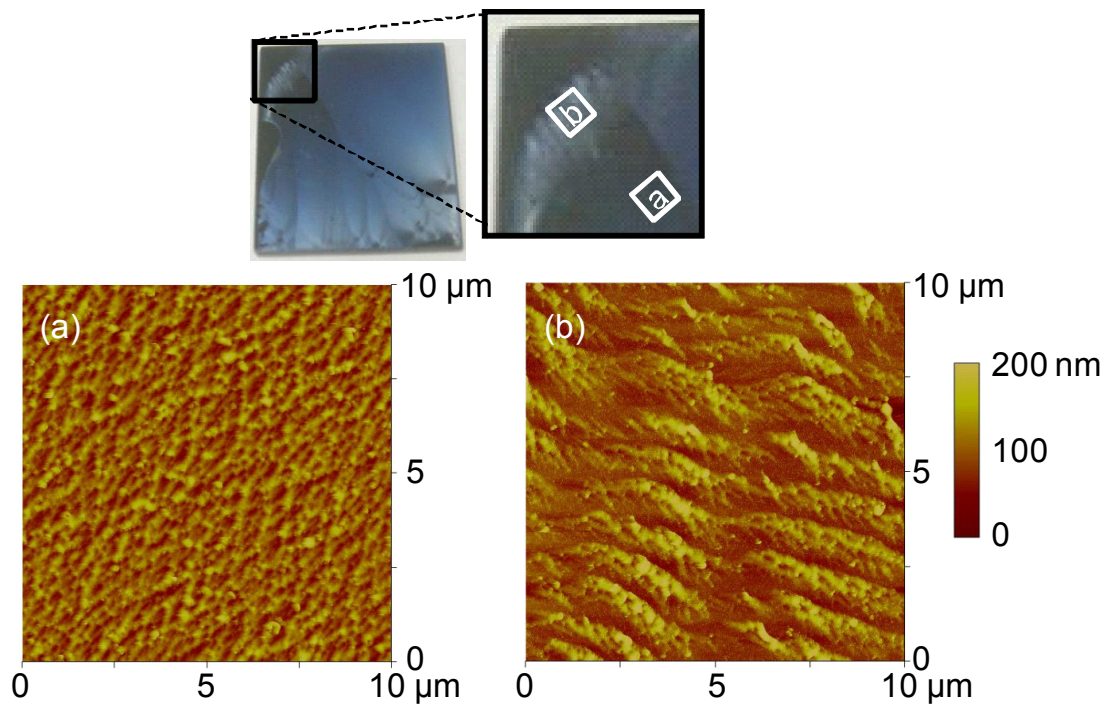


Fig. 3 K. Ohdaira *et al.*,

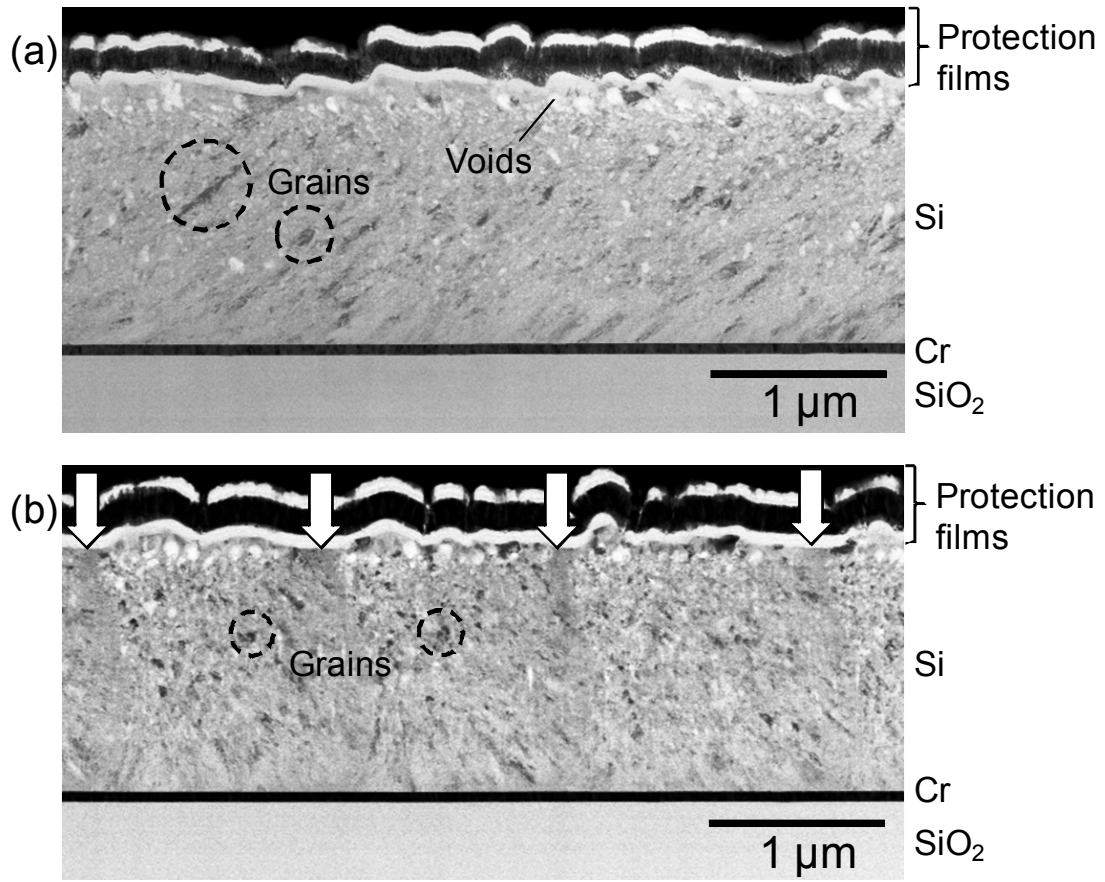


Fig. 4 K. Ohdaira *et al.*,

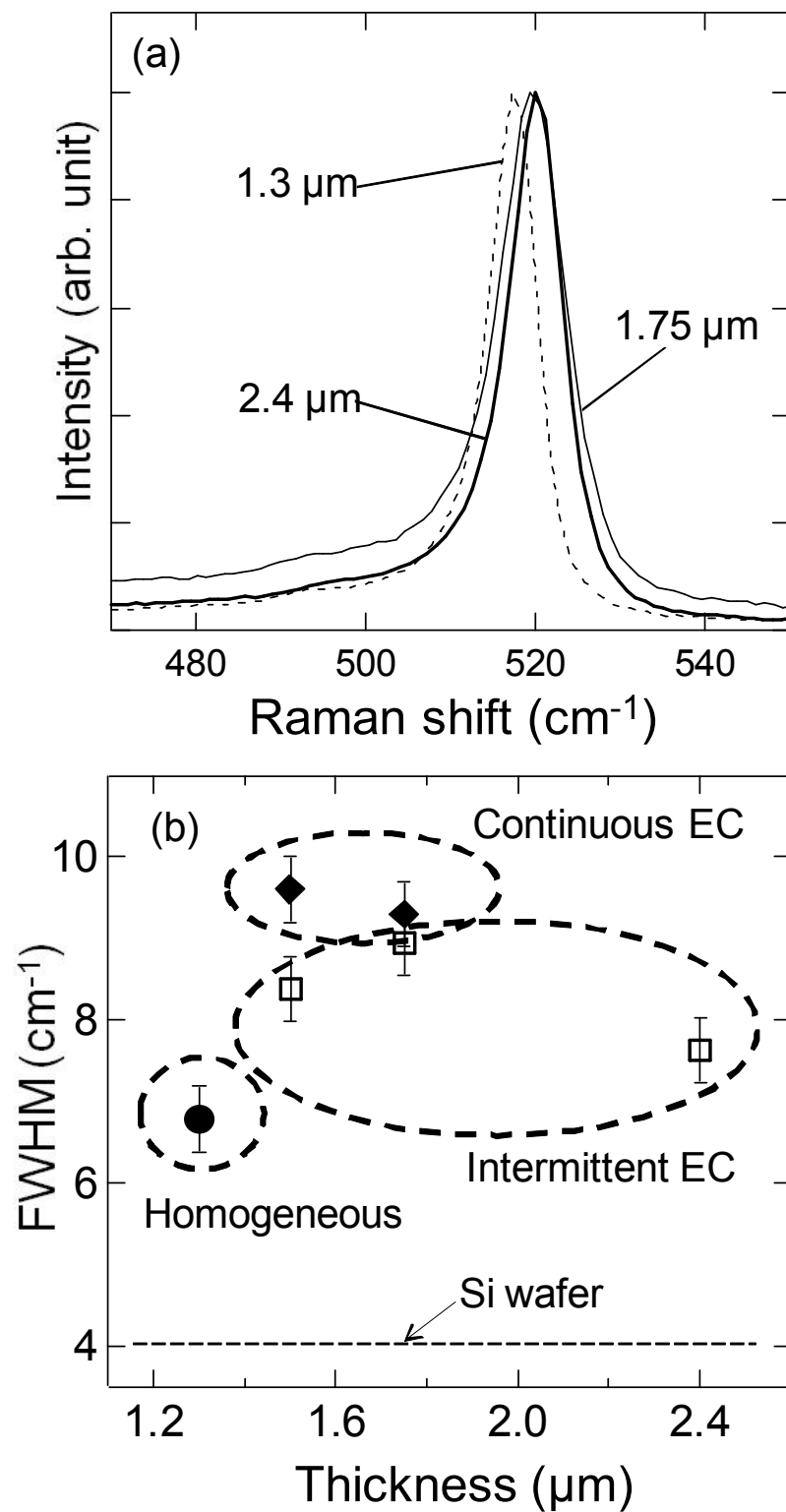


Fig. 5 K. Ohdaira *et al.*,

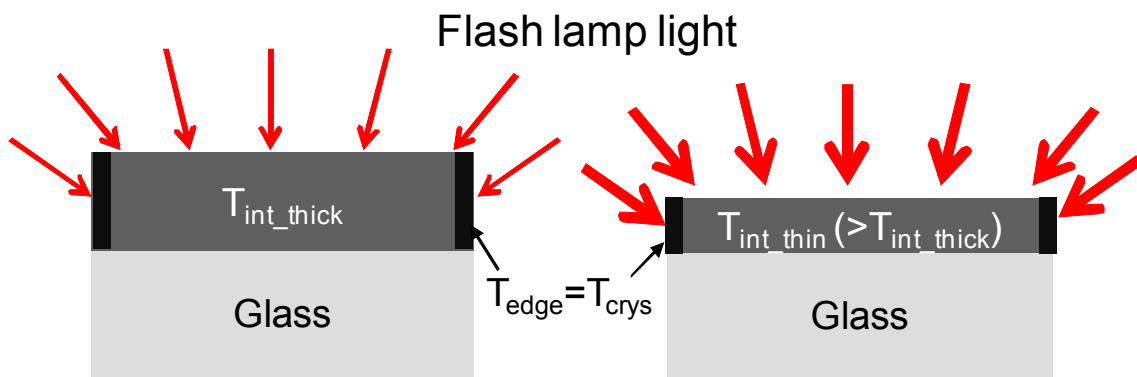


Fig. 6 K. Ohdaira *et al.*,

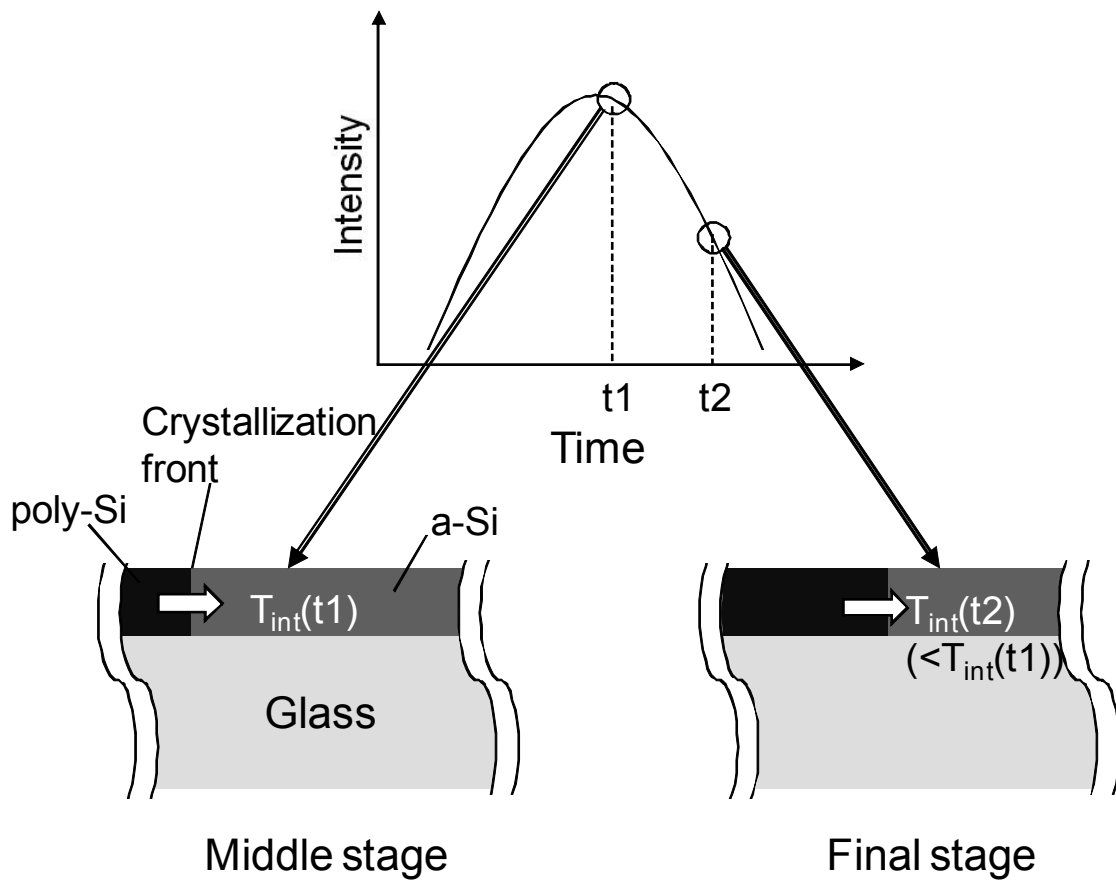


Fig. 7 K. Ohdaira *et al.*,